Spectral Gradients and u-v Sampling

Mark R. Swain

ABSTRACT

I describe a systematic method for characterizing the effects of differences in u-v coverage in terms of inferred spectral gradients in interferometric images. This method is directly applicable to optical and radio interferometry; it is useful in situations when observations using scaled arrays are not feasible.

Subject headings: techniques: interferometric, image processing

[1]Jet Propulsion Laboratory, 4800 Oak Grove Dr., MS 171-113, Pasadena, CA 91109-8099, e-mail: swain@huey.jpl.nasa.gov

1. Introduction

Astronomical interferometers are designed to measure the structure of the spatial coherence function produced by celestial objects. This is traditionally done by measuring the correlated signal on a baseline between pairs of elements in an ensemble of telescopes and allowing the earth's rotation to evolve the projected orientation of the baseline, relative to the celestial source, as a function of time.

The correlated signals between pairs of interferometer elements are termed visibilities; these are a measure of specific components of the spatial coherence function. At radio and submillimeter wavelengths, coherent detectors are used to measure the visibility, V, directly; at optical and infrared wavelengths, the phase noise of the atmosphere is sufficiently large that V^2 is typically measured.

Through the Van Citert-Zernike theorem, measurements of the spatial coherence function may be related to the sky brightness distribution. Taking the Fourier transform of the visibilities directly, model fitting, or some combination are the traditional ways of inferring a sky brightness distribution from the visibility data. In the case of the Fourier transform, deconvolution methods are frequently applied to remove image plane artifacts due to the finite sampling of the spatial coherence function.

The sensitivity of an interferometer to emission from specific angular scales is proportional to the range of baseline lengths and position angles present in the data. The baseline length is measured by the separation of the telescope pair in units of waves. Thus, observing at a shorter wavelength means longer effective baselines and therefore sensitivity to smaller angular scales of source emission.

2. Motivation

Once an interferometer has observed a source at more than one wavelength, there is a strong temptation to use these data to infer information about the spectral properties of the source. The difficulty here is that unless the interferometer baselines were scaled by the wavelength for each observation, the spatial coherence function of the source has been measured in a different way at each wavelength. This leads naturally to an ambiguity: are apparent changes in the source as a function of wavelength due to properties of the source or properties of the measurement?

One would like to sample the spatial coherence function in approximately the same way at a variety of wavelengths. Designing interferometers that can accommodate this observing mode, termed "scaled" arrays, was originally conceived by Martin Ryle (Bridle, A. H. 1998).

Some radio interferometers, such as the Very Large Array (Thompson et al. 1980), the Australia Telescope (Frater el al. 1992), and the Westerbork Synthesis Array (Hogbom & Brouw 1974), are designed to support scaled array observations by moving the antennas. However, scaled array observations restrict the possible combinations of observed wavelength, angular resolution, and spatial frequency dynamic range. Further, many interferometers cannot make scaled array observations because it is simply impractical to move the telescopes.

Because of the instrument and observing limitations associated with scaled array observations, the modern approach to this problem is to sample the *u*-*v* plane as densely as possible, deconvolve, and then convolve the resulting images at different wavelengths to a common angular resolution. Deconvolution effectively interpolates the data into unsampled regions of the *u*-*v* plane. The ability of deconvolution algorithms to interpolate correctly depends on how the *u*-*v* data are weighted, the deconvolution algorithms used, the *u*-*v* sampling density, and the details of the source structure. *Thus, some portions and scales of a source may be more accurately represented than others.* The relevant question for this technique is, given a specific source, what features of a spectral image are artifacts due to *u*-*v* sampling differences? This question has been examined by Lobanov (1997) using an analysis based on the noise in individual images. I describe a systematic method for estimating the effects of *u*-*v* coverage differences, in the presence of noise, on spectral images.

3. Discussion

3.1. The Method

I begin by assuming that a source has been observed with an interferometer at two wavelengths, λ_1 and λ_2, with sampling functions, S_1 and S_2, resulting in visibility data sets, V_1 and V_2; I further assume that V_1 and V_2 have been fully calibrated and that deconvolved images, I_1 and I_2, have been produced.

Given a sparse aperture telescope, we can never know the "true" visibility, $\mathrm{V}(u, v)$, and intensity, $\mathrm{I}(x, y)$, distributions for an extended source. Thus, we cannot construct the "true" spectral image. However, we can ask the question: "does S_1 adequately sample V_2, and does S_2 adequately sample V_1, given a particular level of fidelity in a spectral image constructed with I_1 and I_2?" We can quantitatively answer this question; if the answer is "yes," then a spectral image made from I_1 and I_2 is valid to a particular (and known) level.

Conceptually, the approach is to "resample" the visibility data at one frequency with the sampling function from another. An image, $I_1^{'}$, of the resampled data can then be made using the same method (deconvolution parameters) used to produce the original I_1 image. Differences between the resampled and original image result from the differences in u-v sampling at λ_1 and λ_2. After determining the size of the intensity fluctuations that would produce significant spectral artifacts (given by the sorts of questions the data will be used to answer), a mask can be made by taking $I_1^{'}/I_1$ and setting pixel values equal to zero when they are above or below a value that will yield unacceptably large spectral errors.

I summarize this process as follows. Given that we already have produced

$$I_1(x,y) = D[F[V_1(u,v)]] \tag{1}$$

and

$$I_2(x,y) = D[F[V_2(u,v)]], \tag{2}$$

where D and F represent deconvolution and Fourier transform operations, respectively, we can construct

$$I_1'(x,y) = D[F[S_2(u,v) \times V_1(u,v)]] \tag{3}$$

and

$$I_2'(x,y) = D[F[S_1(u,v) \times V_2(u,v)]]. \tag{4}$$

Where

$$I_1(x,y) \approx I_1'(x,y) \tag{5}$$

and

$$I_2(x,y) \approx I_2'(x,y) \tag{6}$$

are true, a spectral image is valid. Equations 5 and 6 can be tested explicitly on a pixel-by-pixel basis using

$$I_1 ij = I_1' ij \pm \epsilon \tag{7}$$

and

$$I_2 ij = I_2' ij \pm \epsilon, \tag{8}$$

where ϵ corresponds to a particular level of error the astronomer is willing to accept. Thus, if Equations 7 and 8 are true for any pixel ij, then the corresponding pixel in the spectral image is unlikely to contain a false spectral component (greater than some amount corresponding to ϵ) due to differences in u-v sampling.

The above process can be broken down into the following steps, which can be easily undertaken in the Astronomical Imaging Processing System, (AIPS):

1. "Dirty" images from V_1 and V_2 are fully deconvolved (down to the noise in the case of the CLEAN algorithm (Hogbom 1974)) to yield I_1 and I_2.
2. The deconvolution model, M_2, associated with producing I_2, is subtracted from V_2.
3. M_1 is restored to V_2 to create a resampled u-v data set $V_1^{'}$.
4. $V_1^{'}$ is imaged identically to V_1 to produce $I_1^{'}$.
5. $I_1^{'}$ is divided by I_1 to produce a ratio image, R.
6. Pixel values in R are set to zero if $R_{ij} > 1 + \epsilon$ or $R_{ij} < 1 - \epsilon$, where ϵ is computed from the change in I_2 necessary to cause a spectral error $\geq \psi$ where ψ is specified by the astronomer. Remaining pixels in R are set to unity.

Note that step two results in a data set which is the sampling function plus noise. This is important since it ensures that spectral uncertainties associated with the noise, in addition to those due to differences in u-v sampling, will be reflected in R. Multiplying the spectral image by the masks made from I_1'/I_1 and from I_2'/I_2 removes those portions of the spectral image that correspond to insufficiently sampled components of the u-v data.

As an example of an application of this technique, I show some VLA images of the radio galaxy 3C 353 (Swain, Bridle & Baum 1998). The source was imaged with multiple VLA configurations at 1.4, 4.9, 8.4, and 14.9 GHz with the intent of making spectral index images to measure spectral gradients in the source. To assess the gross errors in representing large-scale emission arising from possibly inadequate short-spacing u-v sampling at 4.9, 8.4, and 14.9 GHz, the following comparison was made.

The 1.4 GHz u-v data set was duplicated and u-v data were removed if they corresponded to spacings shorter than the shortest contained in the 4.9, 8.4, and 14.9 GHz data sets, respectively; these "pseudo" 4.9, 8.4, and 14.9 GHz data were then imaged with the same resolution and contoured identically (see Figure 1). From a comparison of the resulting images it is immediately evident that the "pseudo" 14.9 GHz data, and thus by inference the actual 14.9 GHz data, inadequately sample the largest scale of emission in 3C 353 (corresponding to the inner portion of the u-v plane). Although the "pseudo" 8.4 GHz image looks nearly identical to the 1.4 GHz image, this comparison does not guarantee that the actual 8.4 GHz data has done an adequate job of sampling the largest scales of emission present in 3C 353; this is because the "pseudo" data-based comparison made here accounts only for the inner *limit* to the u-v sampling at 8.4 GHz and not for the 8.4 GHz data sampling *density* in the u-v plane.

To determine what portions of 3C 353 were poorly represented (if any) at 8.4 GHz by reduced sampling density in the inner portion of the u-v plane, I applied the resampling technique described above, using the actual 1.4 and 8.4 GHz data, to produce the mask shown in Figure 2. The value of ϵ was chosen to correspond to spectral index errors greater than 0.1. In the upper and lower center regions of the source, there are some regions that would produce spectral index errors at this level and are therefore blanked by the mask.

This example serves to illustrate the point that simply convolving images at different wavelengths to the same resolution, which is the image plane equivalent of removing u-v data falling beyond some radius in the u-v plane, does not guarantee that significant errors in spectral images will not be made. Generally speaking, the more sparsely sampled the u-v data, the larger and more pervasive the errors in spectral images. However, the resampling method described above provides a quantitative test for determining which regions of a source will produce spectral errors of a given amplitude due to inadequate u-v sampling and image noise.

3.2. Optical Interferometers and Imaging

Synthesis imaging has only just begun in optical interferometry and is in a state of relative infancy when compared to the state of the art possible with radio interferometers. Among optical interferometers, only the Cambridge Optical Aperture Synthesis Telescope (Baldwin et al. 1994) and the Navy Prototype Optical Interferometer (Armstrong et al. 1998) have produced synthesis images (Baldwin 1996, Benson et al. 1997). In addition, the Keck Interferometer (Colavita, M. M. 1998, Vasisht, G. 1998), CHARA (McAlister, et al. 1994), and the Very Large Telescope Interferometer (Mariotti et al. 1998), all of which are currently under construction, are all intended to have imaging modes. Even when imaging with optical interferometers is "routine" in a few years, sparse u-v sampling will remain a significant limitation. The temptation to make inferences about the spectral properties of source components will be strong; these inferences should be tempered by a consideration of the artifacts arising from (rather limited) u-v coverage.

There is no substitute for actually measuring the u-v data we require; the above method only provides a systematic way to estimate some of the errors associated

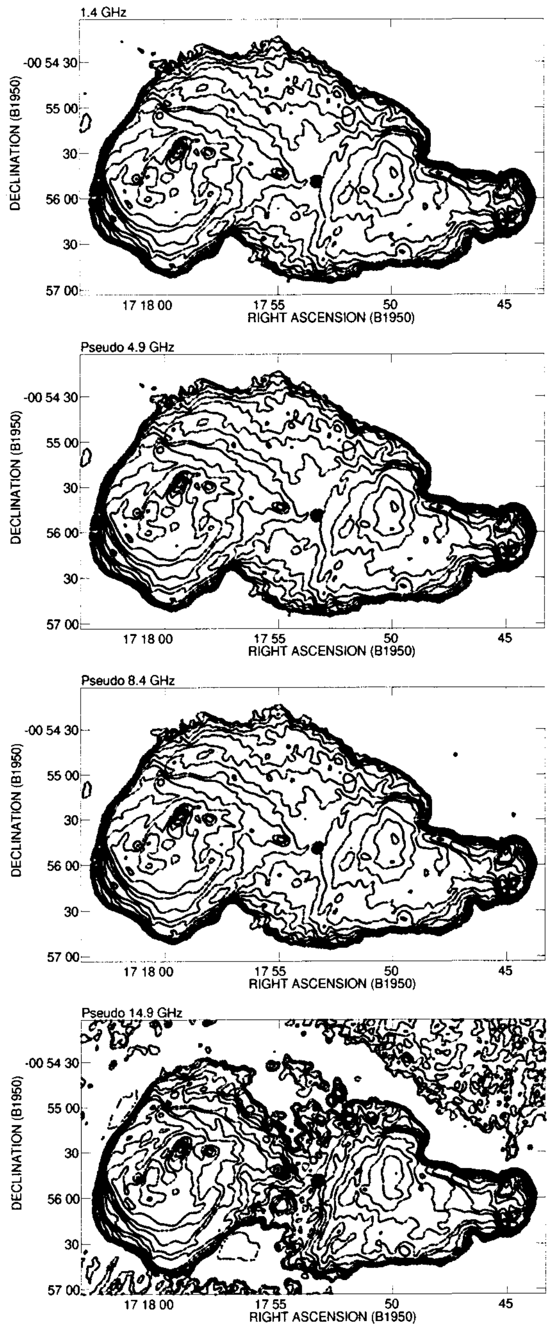

Fig. 1.— 1.4 GHz, 3."0 resolution, images of 3C 353 deconvolved and contoured identically but having different inner u-v limits corresponding to the shortest measured u-v spacings at 1.4, 4.9, 8.4, and 14.9 GHz, respectively. Apparently, the short spacing u-v sampling is insufficient at 14.9 GHz to represent large-scale emission accurately.

Fig. 2.— A mask of pixels with values 1 (grey) or 0 (white) prepared by the method described herein; the scale and directions are the same as in Figure 1. The mask blanks portions of the image which, due to inadequate u-v sampling, would cause spectral index errors of 0.1 or greater. White areas in the central portion of the upper and lower edges of the source indicate regions where the 8.4 GHz data have not adequately sampled the large-scale structure given a limitation of 0.1 on spectral index errors.

with failing to do this. An instrument with a sparse sampling function generally will be very restricted in the types of spectral images it can make. This is unfortunate because spectral information contains a wealth of physical information.

4. Conclusions

While there is no substitute for u-v sampling, scaled array data is likely to be the exception rather than the rule given the design limitations of most interferometers. Deconvolution and approximately similar u-v sampling can effectively duplicate scaled array observations in the dense u-v coverage limit. The method I describe provides a means to test whether the u-v sampling is sufficiently dense for the spectral accuracy required. In cases where there is limited u-v coverage, the technique is particularly useful and provides a systematic method for characterizing the limitations in spectral information that can justifiably be inferred from the observations.

I thank Alan Bridle for valuable discussions regarding the effects of u-v sampling. I thank Gautam Vasisht and Rachel Akeson for their comments on this manuscript. I also thank the referee for assisting in the clarifying of this material. This work has been supported in part by the Jet Propulsion Laboratory.

REFERENCES

Armstrong, J. T. et al. 1998, ApJ, 496, 550

Baldwin, J. E. et al. 1994, Proc. SPIE, 2200, 118

Baldwin, J. et al. 1996, AA, 306, L13

Benson, J. A. et al. 1997, AJ, 114 (3), 1221

Bridle, A. H. 1998, priviate communication

Colavita, M. M. 1998, Proc. SPIE Vol. 3350, p. 776-784, Astronomical Interferometry, Robert D. Reasenberg; Ed.

Frater, R. H. et al. 1992, Journal of Electrical and Electronics Engineering, Australia, Volume 12, no. 2

Hogbom, J. 1974, ApJSS, 15, 417

Hogbom, J. A., & Brouw, W. N. 1974, AA, 33, 289

Lobanov, A. 1997, A&ASS, 132, 2, 261

Mariotti, J.-M. et al. 1998, Proc. SPIE Vol. 3350, p. 800-806, Astronomical Interferometry, Robert D. Reasenberg; Ed.

McAlister H. A., Bagnuolo, W. G., ten Brummelaar, T., Hartkopf, W. I., Turner, N. H., Garrison, A. K., Robinson, W. G., & Ridgeway, S. T. 1994, Proc. SPIE Vol. 2200, p. 129-139, Amplitude and Intensity Spatial Interferometry II, James B. Breckinridge; Ed.

Swain, M. R., Bridle, A. H., & Baum, S. A. 1998, ApJ, 507, L29

Thompson, A. R., Clark, B. G., Wade, C. M., & Napier, P. J. 1980, ApJSS, 44, 151

Vasisht, G. 1998, Proc. SPIE Vol. 3350, p. 354-361, Astronomical Interferometry, Robert D. Reasenberg; Ed.

This 2-column preprint was prepared with the AAS LaTeX macros v4.0.